Quantum Electronics **47** (1) 38–41 (2017)

INTERACTION OF LASER RADIATION WITH MATTER https://doi.org/10.1070/QEL16259

Angular distribution of electrons directly accelerated by an intense tightly focused laser pulse*

O.E. Vais, S.G. Bochkarev, S. Ter-Avetisyan, V.Yu. Bychenkov

Abstract. **We report a study of spectral and angular distributions of electrons directly accelerated from an ultrathin nanofoil by a tightly focused, relativistically intense laser pulse. The approach applied is based on a realistic model describing the focusing of radiation by an off-axis parabolic mirror, the field distribution being simulated with the help of Stratton–Chu integrals. We have compared spectral and angular electron distributions for laser pulses having Gaussian transverse and rectangular intensity profiles on the mirror at the same laser pulse energy. It is shown that in the case of a pulse with a rectangular intensity profile, the energy of fast electrons is higher and the emission angles are smaller than those in the case of a pulse with a Gaussian profile.**

Keywords: *tightly focused relativistically intense laser pulse, direct acceleration of electrons.*

1. Introduction

Modern laser technology aimed at obtaining high-power ultrashort laser pulses makes it possible to produce a large spatiotemporal energy concentration under tight (or ultratight) focusing of a laser beam. When the focal spot diameter becomes comparable to the laser radiation wavelength $\lambda \approx 1$ μm, the peak power can reach several petawatts [1–3] and the intensity up to 2×10^{22} W cm^{-2} [1]. These laser pulses with such extreme characteristics (extreme light pulses) are used for electron and ion acceleration, generation of secondary electromagnetic radiation and initiation of nuclear and thermonuclear reactions [4, 5]. For relativistically intense laser fields, the use of traditional methods of evaluating the characteristics of a laser pulse becomes challenging, which makes it relevant to the search for new methods. One of the possible methods for evaluating the intensity of relativistically intense laser radiation is based on the measurement of the characteristics of electrons directly accelerated by laser radiation from a rarefied gas [6] or an ultrathin foil.

Usually, theoretical studies in this field are based on the paraxial approximation for a laser beam (see, e.g., [7]); however, in the case of tight (ultratight) focusing, it turns out to be beyond the area of applicability of such studies. To correctly describe the propagation of tightly focused pulses, one can use solutions to the Helmholtz equation obtained by the spectral method [8–10] or on the basis of diffraction integrals [10, 11]. It should be noted that the generation of extreme light pulses is only possible under tight (ultratight) focusing of laser light; therefore, to predict the results of experiments one should use a realistic model of laser beam focusing by an off-axis parabola with allowance for nonparaxial field components in the focal region and the real size of the mirror. In addition, an important role is played by the transverse field distribution of the laser beam on the focusing mirror.

It is well known that the transverse intensity profile greatly affects the characteristics of directly accelerated electrons, and by choosing the intensity profile, it is possible to control the characteristics of the laser-accelerated particles [12]. For example, by selecting radially polarised radiation with a minimum of intensity on the axis and a maximum of intensity at the periphery, one can increase the energy of the accelerated electrons and their collimation (see, e.g., [13]).

The purpose of this paper is to describe angular characteristics of electrons produced using their direct acceleration by an intense laser pulse with allowance for the complex structure of the fields in the focal region of an off-axis parabolic mirror. We compare the characteristics of electrons directly accelerated by laser pulses with different initial distributions of fields, namely with Gaussian and rectangular intensity profiles on a parabolic mirror, and in the case of a paraxial Gaussian beam.

2. Model describing direct acceleration of electrons from a thin foil

We will use the Stratton–Chu integral [14, 15] to describe the focusing of a linearly polarised (along the x axis) laser pulse propagating along the optical z axis of a parabolic mirror. As a result of transformations taking into account the shape of the mirror surface, $z = (x^2 + y^2)/(4F) - F \equiv F(s-1)$, the field at point Q with coordinates x_1, y_1, z_1 can be calculated by the formula

$$\hat{\boldsymbol{E}} = \frac{1}{2F\lambda}\iint\left(\mathrm{i}\boldsymbol{A}_\mathrm{e} + \frac{\boldsymbol{a}_\mathrm{e}}{kr_\mathrm{QS}}\right)\frac{\tilde{E}_x}{r_\mathrm{QS}^2}\exp(\mathrm{i}kl)\,\mathrm{d}x\mathrm{d}y, \qquad (1)$$

where $\tilde{E}_x = g(ct + z)E_{0x}(x, y)\exp[-\mathrm{i}(kz + \omega t + \varphi_0)]$ is the field of an electromagnetic wave incident on the surface of the mirror; $E_{0x}(x, y)$ is the spatial distribution of the field amplitude

* Presented at ECLIM2016 (Moscow, 18–23 September 2016).

O.E. Vais, S.G. Bochkarev, V.Yu. Bychenkov P.N. Lebedev Physics Institute, Russian Academy of Sciences, Leninsky prosp. 53, 119991 Moscow, Russia; e-mail: bochkar@lebedev.ru;
S. Ter-Avetisyan Center for Relativistic Laser Science, Institute for Basic Science (IBS), and Department of Physics and Photon Science, Gwangju Institute of Science and Technology (GIST), Gwangju 61005, Republic of Korea; e-mail: sargis@gist.ac.kr

Received 23 November 2016
Kvantovaya Elektronika **47** (1) 38–41 (2017)
Translated by I.A. Ulitkin

on the mirror; $g(ct + z)$ is a slowly varying function of time, which is responsible for the temporal envelope of the laser pulse; c is the speed of light; k, λ, ω and φ_0 are the wave number, wavelength, frequency and initial phase of the laser pulse; F is the focal length of an on-axis (parent) parabolic mirror; $\boldsymbol{A}_e = (2Fr_{QS} - x\Delta x_{QS}, -x\Delta y_{QS}, x(r_{QS} - \Delta z_{QS}))$; $\boldsymbol{a}_e = (-x\Delta x_{QS}, -x\Delta y_{QS}, -x\Delta z_{QS})$, $kl = -kF(s - 1) + kr_{QS}$; and $\boldsymbol{r}_{QS} = (\Delta x_{QS}, \Delta y_{QS}, \Delta z_{QS}) = (x - x_1, y - y_1, z - z_1)$ is the radius vector from point Q to point S with coordinates x, y, z on the mirror surface.

Figure 1 shows a schematic of radiation focusing by a parabolic mirror. The expression for the magnetic component of the electromagnetic field of a focused laser pulse is easily obtained from (1) by replacing the coefficients, i.e., $\boldsymbol{A}_e \to \boldsymbol{A}_b$, $\boldsymbol{a}_e \to \boldsymbol{a}_b$, where $\boldsymbol{A}_b = (-x\Delta y_{QS}, -2F\Delta z_{QS} + x\Delta x_{QS}, 2F\Delta y_{QS})$ and $\boldsymbol{a}_b = -\boldsymbol{A}_b$. The integration in formula (1) is carried out within the projection of the mirror on the xy plane, which in the case of an off-axis mirror can be represented in the form $(x - h)^2 + y^2 \leqslant \rho^2$, where h is the distance between the central axes of the off-axis and parent parabolas (Fig. 1), and ρ is the radius of the mirror, which is selected such that 99% of the laser pulse power is incident on the mirror surface. Note that, in contrast to [15], we do not resort to a simplification associated with the decomposition of the phase kl in formula (1) in the small parameter (the ratio of the distance from the focal point to the observation point to the focal length), without restricting ourselves to the description of the fields exclusively near the focal plane. The temporary shape of the laser pulse will be given in the form $g(ct + z) = \Theta[1 - |kz + \omega(t - \tau)|(\omega\tau)^{-1}] \times \cos^2\{(\pi/2)[kz + \omega(t - \tau)]/(\omega\tau)\}$, where τ is the total duration of the laser pulse, and Θ is the Heaviside function. The field of the pulse incident on the mirror was set as a Gaussian spatial distribution,

$$E_{0x}(x, y) = E_0 \exp\left[-\frac{(x - h)^2 + y^2}{2\rho_0^2}\right], \quad (2)$$

where E_0 is the amplitude of the laser wavelength, and ρ_0 is the radius of the spot on the mirror, or in the form of a stepped distribution,

$$E_{0x}(x, y) = E_0 \Theta\left[1 - \frac{(x - h)^2 + y^2}{\rho^2}\right]. \quad (3)$$

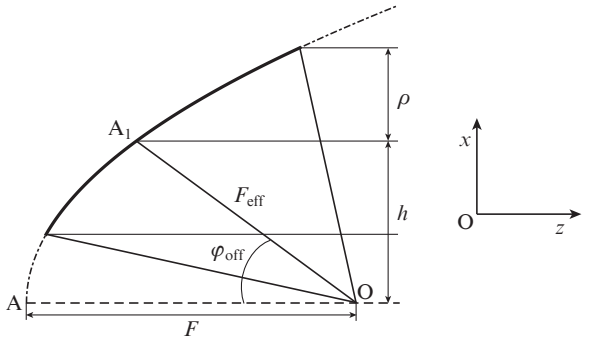

Figure 1. Schematic of focusing of a laser pulse by an off-axis parabolic mirror:
ρ is the mirror radius; point O is the focus of the parabola; F is the focal length of the parent parabola (AO segment); h is the distance from the optical axis of the parent parabola to the parallel line passing through the centre of the mirror A_1; F_{eff} is the effective focal length (A_1O segment); φ_{off} is the off-axis angle.

Based on the shape of the incident beam, we introduce the parameter $f = F_{eff}/(2\rho_0)$, similar to the paraxial case (F_{eff} is the effective focal length of the off-axis parabola, see Fig. 1).

In what follows, we will use, for convenience, the primed coordinate system $x'y'z'$, obtained by rotating the system xyz by an angle of φ_{off} in the xz plane, i.e., $x' = x\cos\varphi_{off} + z\sin\varphi_{off}$, $z' = -x\sin\varphi_{off} + z\cos\varphi_{off}$, $y' = y$. Figure 2 shows the field distribution in the focal plane. A specific feature of spatial distributions of the beam in the focus calculated from the exact formulas is that the periphery exhibits diffraction rings, which are not taken into account in the paraxial approximation, and the intensity within these rings reaches relativistic values. These diffraction rings in the case of a beam with a rectangular beam intensity profile on the mirror (3) have a greater amplitude and, consequently, contribute significantly to the particle acceleration, which will be shown in Section 3.

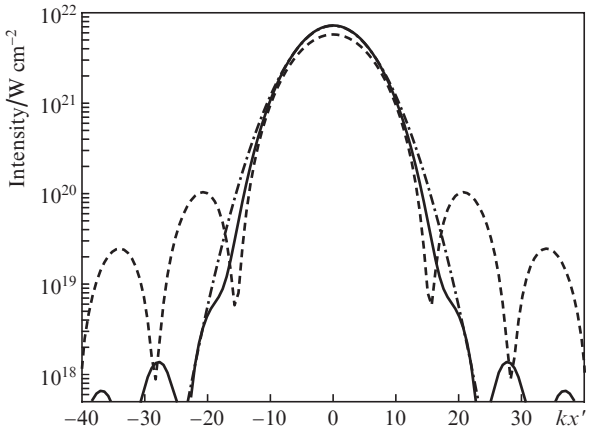

Figure 2. Transverse intensity distributions of the laser pulse in the focal plane, calculated by formulas (1), (2) (solid curve) and (1), (3) (dashed curve) for an off-axis parabolic mirror and in the paraxial approximation (dash-dotted curve) [8].

The dynamics of electrons under the action of a relativistically intense laser pulse emitted from nanofoils can be described by neglecting the plasma fields. This approach allows for a numerical calculation using the method of test particles, which consists in solving the relativistic equation of motion under the action of the Lorentz force:

$$\frac{\mathrm{d}}{\mathrm{d}t} m_e \gamma \boldsymbol{v} = -e\left(\boldsymbol{E} + \frac{\boldsymbol{v} \times \boldsymbol{B}}{c}\right), \quad \frac{\mathrm{d}\boldsymbol{R}}{\mathrm{d}t} = \boldsymbol{v}, \quad (4)$$

where m_e and e are the mass and charge of an electron; $\boldsymbol{R}$, $\boldsymbol{v}$ and γ are the radius vector, velocity and gamma factor of the particle; and the fields $\boldsymbol{E} = \mathrm{Re}\,\hat{\boldsymbol{E}}$ and $\boldsymbol{B} = \mathrm{Re}\,\hat{\boldsymbol{B}}$ are found from formula (1). Here we neglect the self-consistent plasma fields, as well as the influence of the radiation friction force, which is justified for laser intensities $I_F < 10^{23}$ W cm^{-2} [16]. This condition will be considered as one of the limitations of the applicability of our theory.

The use of the probe-particle method naturally restricts the target thickness z. Forces, exerted by the laser pulse on charged particles, must be much greater than the forces caused by plasma fields, which leads to the relationship:

$$\Delta z \ll \frac{a_0 n_{cr}}{\pi n_e} \lambda, \quad (5)$$

where $a_0 = eE_0/(m_e c\omega)$ is the dimensionless amplitude of the field; $n_{cr} = m\omega^2/(4\pi e^2)$ is the critical density equal to 1.7×10^{21} cm^{-3} at $\lambda = 0.8$ μm; and n_e is the density of electrons in the plasma. From relationship (5) it is clear that the smaller the laser pulse intensity, the thinner the foil must be. Thus, the thickness of a carbon (diamond-like) foil at $I_F = 10^{21}$ W cm^{-2} should be less than 18 nm.

3. Dynamics of electrons and comparison of characteristics of accelerated particles

The characteristics of accelerated electrons were analysed for a laser pulse with a fixed energy corresponding to a Gaussian pulse peak power of $P \approx 0.2$ PW, duration of ~30 fs (FWHM) and wavelength of $\lambda = 800$ nm. When calculating by formulas describing the focusing of pulses by a parabolic mirror, we used realistic geometric parameters: spot radius on the mirror $\rho_0 = 15$ cm and the off-axis angle $\varphi_{off} = 60°$, which is defined as the angle between the optical axis of the parent parabola and the segment connecting the centre of the off-axis parabola with its focus (see Fig. 1). For a Gaussian distribution of the incident beam focused by the mirror, the beam waist diameter is $D_F \approx 2\lambda$ for the intensity $I_F \approx 7 \times 10^{21}$ W cm^{-2}, which corresponds to $f = 3.2$ in the calculation by formulas (1), (2) and to $f = 3.75$ for paraxial approximation formulas (with the same value of the focal spot diameter); for the step profile with the same diameter of the focal spot, we have $f = 2$, $I_F \approx 6 \times 10^{21}$ W cm^{-2}. As a computational domain we considered a monolayer located at a distance of the Rayleigh length $z_R = \pi D_F^2/4$ in front of the focal plane measuring $10D_F \times 10D_F$. This choice of the initial position is based on the results of work [9], where it was shown that the optimal initial position of particles is located at this distance. Distributions of accelerated electrons will be characterised by emission angles ϑ and φ in the spherical coordinate system, where the angle ϑ is measured from the axis z' of focused laser pulse propagation, and φ – from the polarisation axis x'. Due to a noticeable effect of the initial phase of the field φ_0, calculations were carried out for its various values. The dynamics of electrons under conditions of tight focusing of a Gaussian pulse has been investigated in [7–9, 17]. We will not consider the trajectories of individual particles and will focus our attention on the comparison of spectral and angular characteristics of electrons at different intensity profiles in the focal spot.

Figure 3 shows angular distributions of accelerated electrons with energies greater than 50 keV. The emission angle is defined in the primed coordinate system: $\vartheta = \arccos(v'_z/v)$. The distribution calculated by exact formulas for a Gaussian spatial profile is narrower compared to that calculated in the paraxial approximation, but in general the two curves vary slightly due to not very tight focusing. The electron acceleration by a beam with a step intensity profile results in a smaller angular distribution corresponding to the maximum of the distribution. This occurs because of the contribution of the diffraction intensity maxima (see Fig. 1) to the expulsion of electrons to the beam axis, i.e. to their collimation, due to the action of transverse ponderomotive forces caused by the transverse gradient of intensity [12]. Thus, this group of electrons is emitted at smaller angles, but the total distribution becomes wider. A wider distribution is again explained by ponderomotive forces tending to force away peripheral electrons in the direction transverse to the laser beam axis.

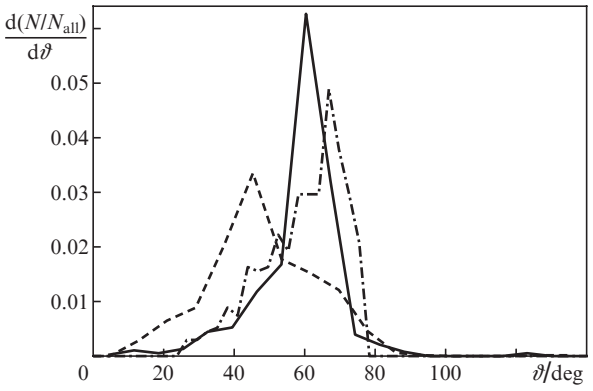

Figure 3. Distributions $d(N/N_{all})/d\vartheta$ of the number of particles with energies above 50 keV over the angle ϑ for pulses with Gaussian (solid curve) and rectangular (dashed curve) intensity profiles, as well as in the paraxial approximation (dash-dotted curve); N_{all} is the total number of particles.

Spectral and angular distributions are highly dependent on the spatial profile of the incident beam. Figure 4 shows the dependences of the finite energy of electrons on the emission angle, where the solid curve shows the analytical curve [17] $\gamma = 1 + 2/\tan^2\vartheta$, corresponding to the approximation of a 'plane' electromagnetic pulse. In focusing a pulse with a Gaussian spatial profile, the emission angles of the particles with small accumulated energy are almost the same as in the case of a plane wave described by an analytic curve (a region up to $\vartheta = 60°$ in Fig. 4). However, at high energies the particle emission angle is shifted relative to this curve. The energies of the particles accelerated by a pulse with a rectangular intensity profile have a larger spread (especially in the region of higher energies) with respect to the analytical curve, even for large angles. Along with an increase in the fraction of fast particles, their energy spectrum changes. Thus, one can see from Fig. 5 that the 'temperature' of the accelerated particles, corresponding to the rectangular intensity profile, is higher than that for the case of Gaussian pulse acceleration. The latter is explained by the fact that due to the peripheral maxima of intensity, fast electrons are emitted in the direction of the axis of laser pulse propagation. These particles stay longer in

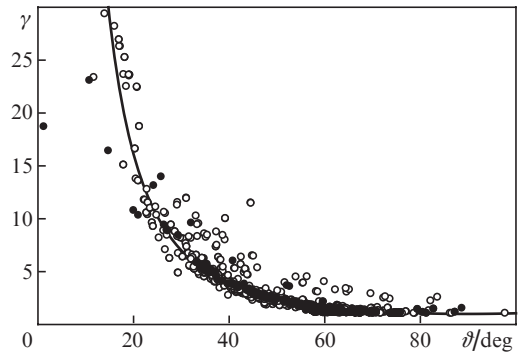

Figure 4. Dependences of the electron energy γ on the emission angle of the particles with energies above 50 keV for pulses with (●) Gaussian and (○) rectangular intensity profiles, as well as the analytical curve (solid curve) [17].

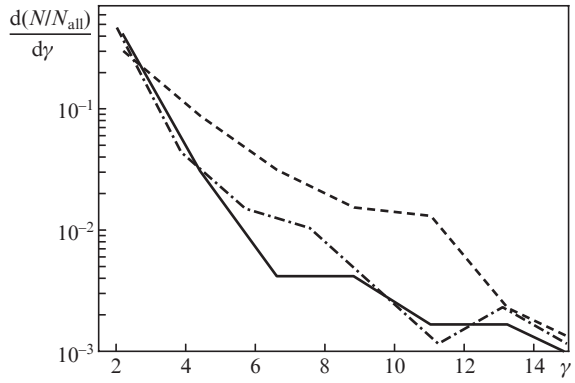

Figure 5. Energy spectra of particles accelerated by a laser pulse, calculated by formulas (1), (2) (solid curve) and (1), (3) (dashed curve) for an off-axis parabolic mirror and in the paraxial approximation (dash-dotted curve) [8].

an intense laser field and, therefore, they are accelerated more efficiently before they propagate a distance equal to the characteristic length of acceleration, i.e. to the Rayleigh length.

To quantify the efficiency of electron acceleration by a pulse with a particular intensity profile, we will analyse the total charges of the particles emitted with an energy of 50 keV from a 5-nm-thick ultrathin foil. When use is made of the paraxial approximation for a Gaussian intensity profile [Eqn (2)], the charge is found to be equal to ~43 nC, which is less than the value of 50 nC obtained using a nonparaxial approach taking into account the shape of the mirror [Eqn (1)]. In the case of a rectangular intensity profile [Eqn (3)] the nonparaxial approach gives a value of the charge of accelerated particles that is several times greater, i.e. about 290 nC. This feature is a consequence of particle acceleration by relativistic peripheral maxima of laser intensity (see Fig. 3). The total charge of the particles with relativistic energies above 1 MeV depends largely on the spatial profile of the incident beam. Its values are equal to 6 and 130 nC for pulses with Gaussian and step profiles, respectively.

Thus, we have studied spectral and angular characteristics of electrons accelerated by laser pulses with Gaussian and step intensity profiles on the mirror under focusing by an off-axis parabolic mirror. To simulate the propagation and focusing of the laser pulse, we have used the Stratton–Chu integral [14, 15], well-known from the vector diffraction theory. The dynamics of electrons is described by the method of probe particles, which imposes a restriction (5) on the foil thickness. We have compared the angular and energy distributions of electrons accelerated from an ultrathin target located parallel to the focal plane at a distance of Rayleigh length. It is shown that the maximum of their angular distribution corresponding to acceleration by a laser pulse with a step spatial profile on the mirror is shifted to lower values of the polar angle and the distribution itself is wider than the distribution of electrons accelerated by a pulse with a Gaussian intensity profile.

The energy spectra of the particles also depend on the intensity distribution of the laser beam on the mirror; for example, the use of a beam with a step intensity profile increases the 'temperature' of the energy spectrum of the accelerated electrons. This feature can be explained qualitatively by ponderomotive forces arising due to a nonmonotonic intensity decrease in a direction transverse to the direction of laser pulse propagation. The influence of the transverse intensity distribution on the particle characteristics is a universal characteristic of direct laser acceleration [12]. Thus, along with the characteristics of nonlinear Thomson scattering of a laser pulse [9], the obtained dependences can form the basis for evaluation of the intensity and quality of the laser beam, including its spatial profile, which will be the subject of a separate publication.

Acknowledgements. This work was supported by the Russian Science Foundation (Grant No. 14-12-00194) and by the Institute for Basic Science (IBS) (Grant No. IBS-R012-D1).

References

1. Yanovsky V., Chuykov V., Kalinichenko G., et al. *Opt. Express*, **16**, 2109 (2008).
2. https://eli-laser.eu/.
3. Yu T.J., Lee S.K., Sung J.H., et al. *Opt. Expres*s, **20**, 807 (2012).
4. Umstadter D. *J. Phys. D: Appl. Phys*., **36**, R151 (2003).
5. Andreev A.V., Gordienko V.M., Savel'ev A.B. *Kvantovaya Elektron*., **31**, 941 (2001) [*Quantum Electron*., **31**, 941 (2001)].
6. Kalashnikov M., Andreev A., Ivanov K., et al. *Laser Part. Beams*, **33**, 361 (2015).
7. Galkin A.L., Kalashnikov M.P., Klinkov V.K., et al. *Phys. Plasmas*, **17**, 053105 (2010).
8. Bochkarev S.G., Bychenkov V.Yu. *Kvantovaya Elektron*., **37**, 273 (2007) [*Quantum Electron*., **37**, 273 (2007)].
9. Vais O.E., Bochkarev S.G., Bychenkov V.Yu. *Fiz. Plazmy*, **42**, 796 (2016); *Kr. Soobshch. Fiz. FIAN*, (12), 62 (2015).
10. Couairon A., Kosareva O.G., Panov N.A., et al. *Opt. Express*, **23**, 31240 (2015).
11. Popov K.I., Bychenkov V.Yu., Rozmus W., Sydora R.D. *Phys. Plasmas*, **15**, 013108 (2008).
12. Stupakov G.V., Zolotorev M.S. *Phys. Rev. Lett*., **86**, 5274 (2001).
13. Bochkarev S.G., Popov K.I., Bychenkov V.Yu. *Fiz. Plazmy*, **37**, 648 (2011).
14. Stratton J.A., Chu L.J. *Phys. Rev*., **56**, 99 (1939); Varga P., Torok P. *J. Opt. Soc. Am. A*, **17**, 2081 (2000).
15. Bahk S.-W., Rousseau P., Planchon T.A., et al. *Appl. Phys. B*, **80**, 823 (2005).
16. Di Piazza A., Hatsagortsyan K.Z., Keitel C.H. *Phys. Rev. Lett*., **102**, 254802 (2009).
17. Quesnel B., Mora P. *Phys. Rev. E*, **58**, 3719 (1998).